Front. Optoelectron. China 2011, 4(2): 156–160
DOI 10.1007/s12200-011-0161-x

RESEARCH ARTICLE

Synthesis and optical property of ZnO nano-/micro-rods

Caixia SONG[1], Yuwei SUN[2], Yaohua XU[2], Debao WANG (✉)[2]

1 College of Materials Science and Engineering, Qingdao University of Science and Technology, Qingdao 266042, China
2 Key Laboratory of Eco-chemical Engineering (Ministry of Education) and College of Chemistry and Molecular Engineering, Qingdao University of Science and Technology, Qingdao 266042, China

Abstract A series of zinc oxide (ZnO) nano-/micro-rods had been synthesized via solution-based routes. In the hydrothermal route, the obtained ZnO nano-/micro-rods had two topographics. In refluxing procedures, spindly ZnO nanorods were obtained in the presence of poly(vinyl-pyrrolidone) (PVP) and ellipsoid-like nanorods were obtained in the absence of PVP. The products were characterized using X-ray powder diffraction (XRD), scanning electron microscope (SEM), transmission electron microscope (TEM), and electron diffraction (ED) analysis. Room temperature photoluminescence (PL) spectra of the ZnO products demonstrated a weak UV emission and a broad visible emission for each of the sample. The growth mechanism of 1-D ZnO crystals was discussed briefly.

Keywords ZnO, nano-/micro-rods, crystal shape, photoluminescence (PL) spectra

1 Introduction

Zinc oxide (ZnO), a direct band-gap oxide semiconductor, has been extensively studied owing to its unique optical, acoustic, and electronic properties, as well as its application in, for example, fabricating electronic and optoelectronic devices [1–3]. Currently, the fabrication of nanomaterials with a controllable size and shape arouse great scientific and technological interest, mainly due to the significant influences of size and shape on their properties. Various interesting 1-D nanostructures of ZnO including nanowire arrays, nanobelts, tetropods, and hierarchical nanostructures have been prepared by vapor transport and condensation process [1–5]. The preparation of ZnO nanowires, nanorods and their arrays via hydrothermal method and chemical solution routes have also been explored [6–10]. The synthesis of ZnO nanorods was carried out in mixed solvent (alcohol/water) in the presence of cetyltrimethylammonium bromide [6]. ZnO nanostructures of different morphologies were grown in a controlled manner through a simple low-temperature hydrothermal method [8]. The effect of crystal growth modifiers on the aspect ratio of ZnO nanorods has been investigated by Garcia's group [10]. However, their explicit growth mechanisms are somewhat controversial and not fully been understood.

Recent studies of liquid-phase synthesis of 1-D nanorods have showed that the growth pattern of nanocrystals is influenced by several different parameters, such as monomer concentration, capping molecules, temperature, and kinetic energy barrier [11]. Understanding the crystal growth behavior would be beneficial to tuning the shape and the orientation of these materials. Herein, in order to clarify the growth behavior, we report the preparation of ZnO 1-D nano-/micro-crystals with tunable size and shape via solution-based routes.

Received November 15, 2010; accepted November 30, 2010

E-mail: dbwang@qust.edu.cn

2 Experimental sections

All the chemicals and reagents were of analytical purity and were used as received. In a typical process, 35 mL $Zn(CH_3COO)_2$ aqueous solution was put into a flask, and pH value was adjusted to 7.0–8.0 with diluted alcohol amine. After being stirred for 1 h, the colloidal mixture was transferred into a Teflon lined stainless steel autoclave with a capacity of 50 mL and was maintained at 120°C for 2 h. Alternatively, the mixture was refluxing at 100°C for 5 h in the flask with or without the presence of poly(vinyl-pyrrolidone) (PVP). The final products were collected by centrifugation, washed with water and dried in vacuum. Controlled experiments were carried out following similar procedures, and typical experimental results are summarized in Table 1.

The X-ray powder diffraction (XRD) pattern of

Table 1 Summary of experimental conditions versus products

No.	Zn^{2+}/(mol/L)	reaction route	temperature/°C	time/h	PVP/%	ZnO products
1	0.0025	hydrothermal	120	2	0.0	ZnO rods
2	0.0067	hydrothermal	120	2	0.0	flower-like rods
3	0.0025	refluxing	100	5	0.0	prolate ellipsoid rods
4	0.0025	refluxing	100	5	1.0	spindly rods
5	0.0067	refluxing	100	5	0.0	ellipsoid rods

the products was recorded by employing a Philips X'pert X-ray diffractometer with Cu Kα radiation (λ = 0.154187 nm). The morphologies and selected-area electron diffraction (ED) of the samples were analyzed using a JSM-6700F field emission scanning electron microscope (SEM) and a JEM-2000EX (JEOL, 160 kV) transmission electron microscope (TEM). The photoluminescence (PL) measurements were performed on a Hitachi 850 luminescence spectrometer at room temperature.

3 Results and discussion

Figure 1 shows XRD patterns of four ZnO samples. The main peaks are labeled and can be indexed to hexagonal wurtzite structure ZnO (JCPDS card No. 36-1451). The strong and sharp peaks suggest the formation of highly crystalline ZnO particles. No characteristic peaks from $Zn(OH)_2$ were observed.

The morphology of the samples was revealed through TEM observations. Figure 2(a) shows the TEM image of sample 1. It can be seen that the sample is mainly rod-like micro-crystals with a diameter of 300–500 nm and length of 3–5 μm. Most of ZnO rods have two detailed topographic features, in which one half part is thicker, and the other half part is thinner. Figure 2(b) shows typical morphology of an individual ZnO micro-rod with not-fully-developed thinner part. Both the thicker and the thinner parts of the rod have the plain shaped ends. It is interesting that the not-fully-developed thinner part seems to be the assemblies of some triangle particles. In fact, triangle shaped particles can be clearly identified in TEM images of Fig. 2. The corresponding ED pattern is shown in the inset of Fig. 2(b), in which the tetragonal pattern could be identified as (0002) and $(11\bar{2}0)$ planes of hexagonal ZnO with the $[1\bar{1}00]$ zone axis projection of the ZnO reciprocal lattice. The ED patterns taken from different positions of an individual rod or from different rods are essentially the same, indicating that ZnO rods are single crystalline in structure. The preferential growth direction of these rods is along the *c* axis of the crystal lattice.

Controlled experimental results showed that the concentration of precursor, reaction route, and capping molecules all have influence on the morphologies of

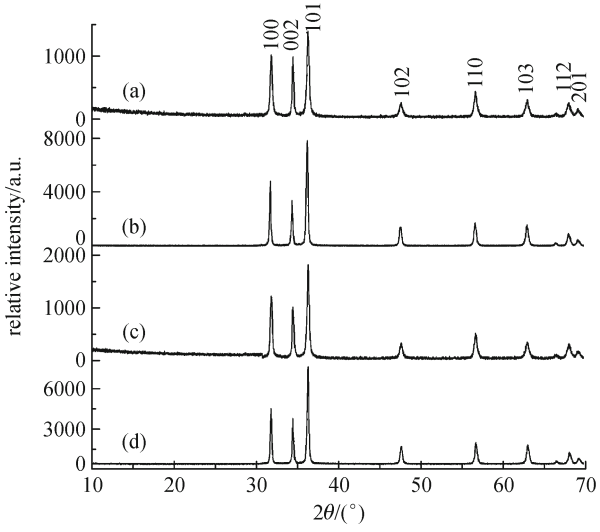

Fig. 1 XRD patterns of ZnO samples. (a) Sample 1; (b) sample 2; (c) sample 3; (d) sample 4

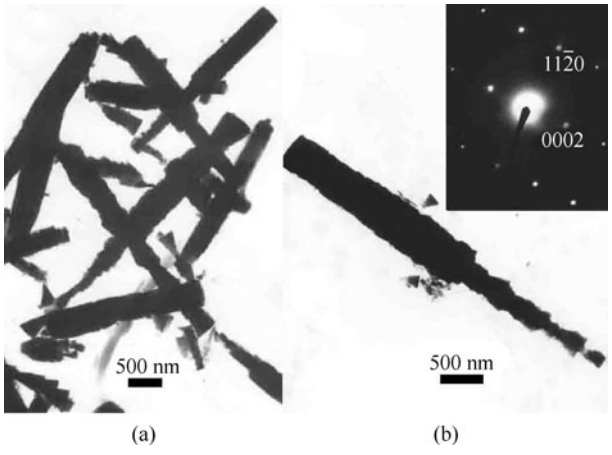

Fig. 2 TEM images and ED pattern (inset of (b)) of sample 1

ZnO crystals. When the concentration of Zn^{2+} was increased (sample 2), uniform ZnO nanorods can be obtained. Figure 3(a) shows the SEM image of sample 2, exhibiting flower-like assemblies. The TEM image in Fig. 3(b) shows that the ZnO nanorods have the diameters of 80–200 nm. When the crystallizing process is carried

out by refluxing the suspension of $Zn(OH)_2$ precursor, prolate ellipsoid-like ZnO rods are obtained (sample 3). As shown in Fig. 3(c), both ends of ZnO rod are pointed. ED pattern in Fig. 3(d) is recorded by focusing the electron beam on an individual ZnO rod, indicating the *c* axis preferential growth behavior of ZnO rods. The slighter spot of (0001) might result from the secondary reflection of (0002) in ZnO crystals. Increasing the concentration of the precursor also results in ellipsoid-like ZnO particles (sample 5). While the precursor was refluxed in the presence of PVP (sample 4), as shown in Fig. 3(e), spindly ZnO crystals with higher aspect ratio are obtained.

The overall reaction for the growth of ZnO crystals may be simplified as the following:

$$Zn^{2+} + 2OH^- \rightarrow Zn(OH)_2, \quad (1)$$

$$Zn(OH)_2 + 2OH^- \rightleftharpoons [Zn(OH)_4]^{2-}, \quad (2)$$

$$[Zn(OH)_4]^{2-} \rightarrow ZnO + H_2O + 2OH^-. \quad (3)$$

Although the chemical reaction is rather simple, the growth process of ZnO nano-/micro-rods would be very complicated because of the fact that the ZnO rods obtained in different conditions show distinguishing morphology characteristic. ZnO crystal is a polar crystal, the inherent asymmetry along *c* axis leads to the anisotropic growth of ZnO crystallites. In hydrothermal process, the growth unit of ZnO is $[Zn(OH)_4]^{2-}$, and it is acceptable that the growth rate of different ZnO planes is as the following: $V(0001) > V(01\bar{1}\,\bar{1}) > V(01\bar{1}0) > V(01\bar{1}1) > V(000\bar{1})$ [12]. As a result, column-like 1-D structured ZnO crystal is

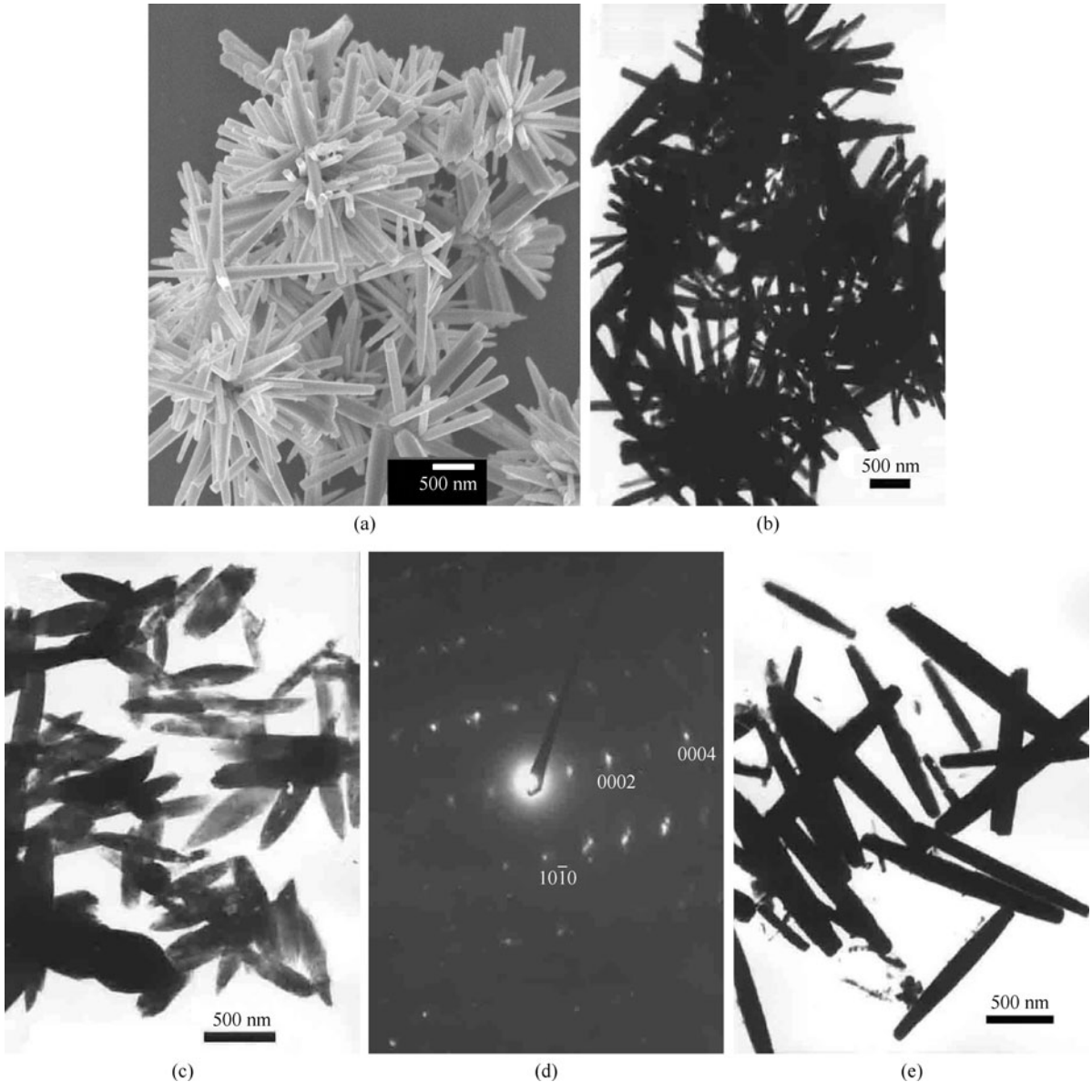

Fig. 3 SEM and TEM images and ED pattern. (a),(b) Sample 2; (c),(d) sample 3; (e) sample 4

formed with one end faceted, and another end pointed or faceted. This kind of ZnO 1-D structure is easy to be found in Refs. [6,13]. However, ZnO nano-/micro-rods obtained in the present case show different growth behaviors.

In our process, some of the ZnO rods show two distinct topographics, and the growth behavior of the thinner half part seems different from that of the thicker half part. We speculate that the rod formation process is as follows: When the reaction takes place, ZnO nuclei take form according to reaction formula (3). The growth units of $[Zn(OH)_4]^{2-}$ are generated according to reaction formula (2). The assemblis of $[ZnO_4]^{6-}$ tetrahedrons along [0001] direction lead to 1-D growth of ZnO. Under higher concentrations of the precursor (sample 2), more ZnO nuclei take form. The newly formed nuclei might aggregate in the absence of PVP. The radial 1-D growth of ZnO from the aggregated nuclei leads to the formation of flower-like ZnO nanorods arrays.

In the refluxing process, ZnO prolate ellipsoid-like rods with two pointed ends were obtained instead of the column-like ones reported in the literature. We propose that the relative growth rate of different facets is probably not as same as that in the hydrothermal process. The difference of relative growth rate between the [0001] and $[000\bar{1}]$ directions diminishes, and the growth rate in the $[01\bar{1}0]$ direction is also accelerated, which results in the growth of ellipsoid-like ZnO nanorods with two pointed ends. With the assistance of PVP, the growth rate in the $[01\bar{1}0]$ direction is limited, and those in the $[01\bar{1}\,\bar{1}]$ and the $[01\bar{1}1]$ directions are enhanced, which leads to the formation of spindly ZnO nanorods with higher aspect ratio.

Figure 4 shows the room temperature PL spectra of ZnO samples excited with a wavelength of 325 nm. It can be seen that the PL spectra cover the blue and green regions. This kind of broad-peak PL spectrum in a visible region for ZnO nanorods has rarely been reported [14,15]. The sharp and strong UV emission band in previous reports was not recorded in the present case. In contrast, only relatively weak UV emission at around 385 nm was recorded for samples 2 and 4 respectively (Figs. 4(b) and 4(d)). And a 413 nm visible emission was detected for sample 3. Generally, the UV emission band is originated from the direct recombination of the free excitons through an exciton-exciton collision process [16,17], while the visible emission is due to surface structure defects in ZnO crystals such as oxygen vacancies, zinc vacancies, oxygen interstitials, and zinc interstitials [18]. These results indicate that the as-obtained ZnO nanorods have more structural defects. It also suggests that the optical properties of ZnO crystals are sensitive to the size and the morphologies of ZnO samples.

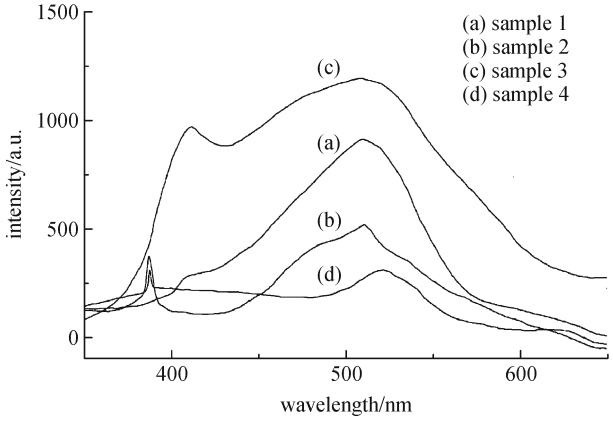

Fig. 4 PL spectra of ZnO samples

4 Conclusions

In conclusion, ZnO nano-/micro-rods of different shapes have been synthesized by decomposing the in-situ formed $Zn(OH)_2$ precursor. The experimental results show that experimental parameters such as the concentration of precursor, reaction route, and capping molecules have influences on the morphologies of ZnO samples. The growth mechanism is discussed, and it would provide more information to the controlled synthesis of 1-D ZnO nano-/micro-crystals. Room temperature PL study indicates that the optical properties of ZnO crystals are sensitive to the size and the morphologies.

Acknowledgements This work was supported by the Natural Science Foundation of Shandong Province (No. ZR2009BL018) and the Foundation of Education Department of Shandong Province (No. J10LB11).

References

1. Huang M H, Mao S, Feick H, Yan H, Wu Y, Kind H, Weber E, Russo R, Yang P. Room-temperature ultraviolet nanowire nanolasers. Science, 2001, 292(5523): 1897–1899
2. Penner R M. Hybrid electrochemical/chemical synthesis of quantum dots. Accounts of Chemical Research, 2000, 33(2): 78–86
3. Wang Z L. Zinc oxide nanostructures: growth, properties and applications. Journal of Physics: Condensed Matter, 2004, 16(25): R829–R858
4. Liu F, Cao P J, Zhang H R, Li J Q, Gao H J. Controlled self-assembled nanoaeroplanes, nanocombs, and tetrapod-like networks of zinc oxide. Nanotechnology, 2004, 15(8): 949–952
5. Wang D B, Song C X. Controllable synthesis of ZnO nanorod and prism arrays in a large area. The Journal of Physical Chemistry B, 2005, 109(26): 12697–12700
6. Zhang H, Yang D, Ji Y, Ma X, Xu J, Que D. Low temperature synthesis of flowerlike ZnO nanostructures by cetyltrimethylammonium bromide-assisted hydrothermal process. The Journal of Physical Chemistry B, 2004, 108(13): 3955–3958
7. Jung S H, Oh E, Lee K H, Yang Y, Park C G, Park W, Jeong S H.

Sonochemical preparation of shape-selective ZnO nanostructures. Crystal Growth & Design, 2008, 8(1): 265–269

8. Pal U, Santiago P. Controlling the morphology of ZnO nanostructures in a low-temperature hydrothermal process. The Journal of Physical Chemistry B, 2005, 109(32): 15317–15321
9. Shen L, Bao N, Yanagisawa K, Gupta A, Domen K, Grimes C A. Controlled synthesis and assembly of nanostructured ZnO architectures by a solvothermal soft chemistry process. Crystal Growth & Design, 2007, 7(12): 2742–2748
10. Garcia S P, Semancik S. Controlling the morphology of zinc oxide nanorods crystallized from aqueous solution: the effect of crystal growth modifiers on aspect ratio. Chemistry of Materials, 2007, 19 (16): 4016–4022
11. Peng X G. Mechanisms for the shape-control and shape-evolution of colloidal semiconductor nanocrystals. Advanced Materials, 2003, 5 (15): 459–463
12. Li W, Shi E, Yin Z. Growth behavior of polar crystals. Chinese Science Bulletin, 1999, 44: 2388–2392 (in Chinese)
13. Hou H, Xiong Y, Xie Y, Li Q, Zhang J, Tian X. Structure-direct assembly of hexagonal pencil-like ZnO group whiskers. Journal of Solid State Chemistry, 2004, 177(1): 176–180
14. Gao P, Ying C, Wang S, Ye L, Guo Q, Xie Y. Low temperature hydrothermal synthesis of ZnO nanodisk arrays utilizing self-assembly of surfactant molecules at solid-liquid interfaces. Journal of Nanoparticle Research, 2006, 8(1): 131–136
15. Gao S Y, Zhang H J, Wang X M, Deng R P, Sun D H, Zheng G L. ZnO-based hollow microspheres: biopolymer-assisted assemblies from ZnO nanorods. The Journal of Physical Chemistry B, 2006, 110(32): 15847–15852
16. Vanheusden K, Warren W L, Seager C H, Tallant D K, Voigt J A, Gnade B E. Mechanisms behind green photoluminescence in ZnO phosphor powders. Journal of Applied Physics, 1996, 79(10): 7983–7990
17. Mitra A, Thareja R K. Photoluminescence and ultraviolet laser emission from nanocrystalline ZnO thin films. Journal of Applied Physics, 2001, 89(4): 2025–2028
18. Usui H. Influence of surfactant micelles on morphology and photoluminescence of zinc oxide nanorods prepared by one-step chemical synthesis in aqueous solution. The Journal of Physical Chemistry C, 2007, 111(26): 9060–9065